12-2017

Increase in the Reduction Potential of Uranyl upon Interaction with Graphene Oxide Surfaces

V. N. Bliznyuk
Clemson University

N. Conroy
Clemson University

Y. Xie
Clemson University

R. Podila
Clemson University

A. Rao
Clemson University

See next page for additional authors

Recommended Citation

Please use the publisher's recommended citation. http://pubs.rsc.org/en/content/articlelanding/2018/cp/c7cp04197g#!divAbstract

Authors
V. N. Bliznyuk, N. Conroy, Y. Xie, R. Podila, A. Rao, and Brian A. Powell

Increase in the reduction potential of uranyl upon interaction with graphene oxide surfaces

V. N. Bliznyuk[1*], N. Conroy[1], Y. Xie[1], R. Podila[2], A. Rao[2], B. A. Powell[1*]

[1] Department of Environmental Engineering and Earth Sciences, Clemson University, Clemson, SC 29634 USA

[2] Department of Physics and Astronomy, Clemson University, Clemson, SC 29634 USA

Abstract

Coordination of uranyl (U(VI)) with carboxylate groups on functionalized graphene oxide (GO) surfaces has been shown to alter the reduction potential of the sorbed uranium ion. A quantitative measure of the reduction potential and qualitative estimation of sorption/desorption processes was determined using cyclic voltammetry and a proposed coordination environment has been determined using surface sensitive attenuated total reflection mode of infrared spectroscopy (ATR-FTIR). GO is a nanostructured material possessing large amount of oxygen containing functional groups on both basal planes and the edges, which can form strong surface complexes with radionuclides. The presence of these functional groups on the surface of GO allows efficient immobilization of uranium due to sorption of uranyl (UO_2^{2+}) to carboxylate, hydroxide, or sulfonate functional groups and the potential for enhanced reduction of U(VI) to more strongly sorbing and insoluble U(IV) . Binding of U(VI) to carboxylate groups on the GO surface is proposed as the primary sorption mechanism based on the FTIR study in this work. Furthermore, the coordination of uranium with the surface increases the reduction potential of the U(VI)/U(IV) redox couple relative to that of aqueous U(VI)/U(IV) species. This is consistent with the alteration of the electronic structure of the sorbed ion, which could be measured in our case due to the GO coated working electrode. Thus, GO coated glassy carbon electrodes and other semi-conducting electrodes with high ion sorption capacities may provide a means of examining the oxidation/reduction potentials of sorbed ions.

KEYWORDS: Graphene oxide; electrochemistry; uranium; adsorption;

Introduction

Nuclear energy remains an important growing segment in the global energy production. Under conditions of a safe usage nuclear power can be considered as an environmentally clean sustainable energy source allowing significant reduction of carbon emission into atmosphere in comparison to traditionally used fossil fuels.[1] At the same time, nuclear power poses potential threats to the environment and society due to the inadvertent exposure to radioactive materials. In addition to naturally occurring uranium ores, considerable amounts of uranium can be eventually released into the environment due to nuclear fuel cycle activities, imposing long-term threats to human beings and bio-organisms.[2] Therefore, an efficient enrichment of uranium, as well as its recovery from waste aqueous solutions is of extreme importance for full utilization of resources and environmental protection.

Solid state extraction of uranium using carbon based materials has been one of the most successful extraction based techniques thus far.[3] Different carbon materials, which have been previously tested for the removal and recovery of uranium from aqueous solutions include the activated carbons and carbon nanotubes (CNTs).[3] Oxidized multi-walled CNTs proved to be effective in the pre-concentration and solidification of U(VI) from large volumes of aqueous solutions.[4] Interestingly, the extraction efficiency for U was highly correlated with oxygen-containing (hydroxyl, carbonyl, or carboxyl) functional groups on the CNT surface. Thusly, the efficient extraction of the metal is primarily due to the surface complexation with aqueous UO_2^{2+} dioxycations.

Graphene oxide (GO) is constituted of oxidized graphene sheets and can be prepared in bulk quantities from graphite through two main approaches known as Brodie and Hummers methods.[5] In the former technique, treatment of graphite with a mixture of potassium chlorate and fuming nitric acid leads to the exfoliation of GO sheets. In the Hummers method, simultaneous delamination and oxidation of graphite into GO occurs when graphite is mixed with sulfuric acid, sodium nitrate and potassium permanganate. Depending on the ratio of oxidizing agents and graphite, the degree of oxidation (i.e., the concentration and type of oxygen containing surface groups) may vary significantly, leading to a broad variation of physical and chemical properties of GO. Recently, additional techniques have been reported for GO with better controlled size and chemical functionality, including those that allow “unzipping” of carbon nanotubes [6] or use the so-called “bottom up” construction of GO sheets from a glucose precursor.[7] As demonstrated in previous studies oxidation of graphene to GO leads to the functionalization of its basal planes with epoxide and hydroxyl groups. In addition, carbonyl and carboxyl groups are produced during GO synthesis which are predominantly located at the edges and defect locations in the graphene sheets. The resulting GO is hydrophilic and can be dispersed in water to form stable colloidal suspensions.

Due to presence of oxygen containing functional groups on the surface, GO possesses the highest adsorption capacity in the removal of divalent metallic ions (like Pb(II), Cd(II), and Co(II)) from water solutions in comparison to any known nanomaterial.[8,9,10] Thus, the maximum reported sorption capacity of a single-layered GO for Cu(II) reaches 46.6 mg/g, which is almost ten times higher than that of any commercially available activated carbon (around 5 mg/g).[11] High affinity of uranyl ions to GO surface has also been demonstrated in several recent publications.[12-16] Maximum sorption capacities of 78 and 298 mg/g were reported for tri- and hexavalent ions Eu(III) and U(VI), respectively.[17]

In this work, we investigate the redox reactions and surface interaction of ^{238}U with GO sheets, and correlate the observed variations in sorption with the chemical and physical structure of the GO. Specifically, we demonstrate how uranyl sorption affinity and the formation of complexes with surface functional groups alter the redox potential of the surface complex relative to the free ions in bulk solution. Furthermore, we confirmed this formation of complexes from the change in the uranium valence state and reduction potential on the oxidized graphene surfaces (through interaction with carboxylate functional groups) by comparing to the well understood reduction of aqueous uranyl carboxylate complexes. Interestingly, we find evidence for this complexation despite the fact that aqueous complexes are not favored in uranyl solutions with a low pH. Lastly, we find that completely delaminated a single-layer or few-layer GO allows for better sorption relative to a multilayer GO material, which exhibits limited sorption due to difficulties in intercalating uranyl complexes between layers held by van der Waal’s forces.

Experimental

The GO2 sample was synthesized in two steps using exfoliation of graphene from graphite followed by a modified Hummer’s method for graphene oxidation to GO.[5,18] First, bulk graphite (~1 g) was dispersed in 100 mL of N-methyl-2-pyrrolidinone (NMP) and sonicated using 1/8” tip sonicator (Branson 250) at 100 W for 2 h. The resulting dispersion was filtered through a 0.45 μm nylon filter and re-suspended in 100 mL of fresh NMP. Subsequently, the solution was bath sonicated for 6 h and centrifuged at 5000 rpm for 45 min. The supernatant was vacuum filtered using a 0.45 μm nylon filter. Finally, the filtered powder was washed five times using deionized water to remove residual NMP. This method was repeated on multiple batches of bulk graphite to obtain ~2 g of exfoliated graphene. At the second step, chemically exfoliated graphene (2 g) was dispersed in concentrated H_2SO_4 (46 mL). $KMnO_4$ (6 g) was added gradually with stirring in an ice bath. The mixture was then stirred at 35°C for 2 h, and deionized water (100 mL) was added. In 1 h, the reaction was terminated by the addition of a large amount of deionized water (300 mL) and 30% H_2O_2 solution (5 mL), causing violent effervescence and an increase in temperature to 100°C, after which the color of the suspension changed to bright yellow. The suspension was washed with 1:10 HCl solution (500 mL) three times in order to remove metal ions by filter paper and funnel. The paste collected from the filter paper was dried at 60°C, until it became agglomerated. The agglomeration was washed five times with deionized water and air-dried to obtain graphene oxide samples (GO2).

Cyclic voltammetry (CV) studies were performed with WaveDriver 20 Bipotentiostat/ Galvanostat using BASi VC-2 voltammetry cell (20 ml) with Ag/AgCl reference and Pt counter electrodes. Argon gas was purged through the cell headspace during CV experiments. Working GO electrodes were prepared by casting thin films of GO particles from water dispersions on the surface of a pre-cleaned glassy carbon electrode (BASi MF-2012). Typical voltage variation was in the range of -0.6 to +1.2V with the sweep rate of 300, 100, 50, 10 and 5 mV/s and recording of 5 scans for each scan rate. In experiments with pre-adsorbed ^{238}U, 1:1 by volume mixtures of 5 mM solution of uranium nitrate (with 0.1 M of sodium perchlorate) and 4 mg/ml dispersion of GO in water were prepared and mixed end-over-end for 24 h at room temperature. The GO phase with adsorbed uranyl ions was then concentrated on the bottom of a testing tube via centrifugation with 10k rpm rotation speed for 15 min. The top fraction (clear water solution without GO particles) was extracted with a pipette and used for mass-spectroscopy monitoring of ^{238}U aqueous concentration using inductively coupled plasma mass spectrometry (ICP-MS, Thermo X Series II). The bottom fraction (black slurry of GO particles) was deposited on top of GC electrode which was inverted and held in a vertical positon so the end of the electrode could be coated. After evaporation of water (typically within 1-2 hours) the electrode was ready for CV experiments. A second set of experiments was performed where uranium-free GC, GO1, and GO2 electrodes were placed into 1mM U(VI) solutions to allow for adsorption of uranium during the CV experiments. Similar to experiments with pre-adsorbed uranium on the eletrodes, these experiments were performed with 0.01 M NaCl as a background electrolyte. Prior to placing the electrode into the U(VI) bearing solution, the electrode was conditioned in 0.01 M NaCl for 1 hour across the range -0.6 V to +1.2 V and a scan rate of 100 mV/s. A peak near 0.8V was observed during this conditioning step which decreased over time and did not re-appear and was attributed to oxidation of carbon monoxide on the GO surface.

Attenuated total reflection mode Fourier transform Infra-Red spectroscopy (ATR-FTIR) was applied to study variation of the chemical composition and sorption of the uranium on the working electrode surface. The GO electrode was placed directly onto a Smart iTR single bounce diamond ATR crystal and analyzed using a Thermo Scientific 6700 FTIR equipped with a mercury cadmium telluride narrow band detector.

The GO samples were characterized using X-ray diffraction, surface area analysis, and elemental analysis. The XRD pattern was measured using a Miniflex X-ray diffractometer (Rigaku, Japan). For BET specific surface area measurement and CHNS elemental analysis, 6 mL of GO stock solution was transferred to a beaker and evaporated with moderate heat (<80 ºC); the dried GO samples were then vacuumed at < 100 ºC in a vacuum oven overnight to remove moisture and impurities in the samples. The BET surface area measurement was performed with a N_2(g) physisorption analyzer (Micromeritics ASAP 2020). The CHNS elemental analysis was conducted with FlashEA 1112 elemental analyzer. BBOT ($C_{26}H_{26}N_2O_2S$) was used as a standard for CHNS quantification.

Results and Discussion

GO obtained from two independent sources were used in this study: a commercially procured Sigma-Aldrich GO (sample ID: GO1) and the one prepared in the lab (sample ID: GO2). To synthesize GO2, graphite was first exfoliated to yield graphene, which was then oxidized to GO by a modified Hummer's method.[18,19] Our x-ray diffraction (XRD) and x-ray photoelectron spectroscopy (XPS) studies revealed distinct variations in the structure and surface functionalization of the two GO samples. Particularly, GO1 sample exhibited an X-ray diffraction peak corresponding to an interlayer spacing of 1.5 nm, which is much higher than in graphite. This is probably due to the preparation technique, which created defects in the graphene precursor to promote intercalation of various species between the graphene sheets. On the other hand, no diffraction peaks were observed for GO2, which is consistent with its few-monolayer nature. BET surface area, specific capacitance (based on CV background current), and distribution of different oxygen containing functional groups (XPS analysis data) in GO samples under study are summarized in Table 1. Lastly, both GO samples contained sulfonic groups which is attributed to the sulfuric acid treatment in the Hummer's preparation method.[18] However, the measured from

XPS analysis content of sulfur is significantly higher in GO2 in comparison to GO1 (13% by mass versus 4%, Supporting Information file).

Table 1. Summary of physical and chemical peculiarities of two GO samples under study.

Physical parameters		
	GO1 (Aldrich)	**GO2 (this study)**
BET surface area	307 m^2/g	50 m^2/g
Area capacitance	5.25 $\mu F/cm^2$	148.5 $\mu F/cm^2$
XRD data	Multilayered particles with 1.5 nm periodicity between layers	single to few layer sheets, amorphous
Relative Abundance of Oxygen Containing Functional Groups Determined using XPS		
	GO1 (Aldrich)	**GO2 (this study)**
Epoxide	16 %	7 %
Phenolic	7 %	17 %
Carboxylic	8 %	12 %

Representative CV curves recorded using glassy carbon (GC) and the two types of GO electrodes during voltammetry experiments with ^{238}U (initially as U(VI) in the aqueous phase) are shown in Figure 1. Oxidation and reduction peaks are marked with arrows. The difference in the shape of the curves corresponds both to the difference in the specific surface area and the nature of functional groups on the surface of GO electrodes. There are two main differences between two GO electrodes. First, the area enclosed by the cyclic voltammogram for GO2, which indicates the double layer capacitance, is significantly higher than GO1 (see Fig. S1 in the supporting information). The double layer capacitance of GO2 in 0.1M NaCl (Fig. S1) was found to be ~48 $\mu F/cm^2$, i.e., significantly higher than GO1 and GC, which showed almost no double layer capacitance. This observation suggests that GO2 has more freely accessible surface area for ion adsorption relative to GO1 and GC. Furthermore, the observation of higher capacitance of GO2 is somewhat counter intuitive based on the higher surface area of GO1 measured using N_2(g) adsorption. However, we propose that N_2(g) adsorption may not fully represent these multilayered materials and that the capacitance measurements are more representative of the surface reactivity and functional groups.

The second difference between the voltammograms of GO1 and GO2 is that a more complex shape with two oxidation peaks (and in some cases with two reduction peaks) was observed for the GO1 working electrode in comparison to the GO2 electrode (Fig. 1). We interpret this as having two different chemical species of uranium near or at the surface of the electrode. One is based on ionic U(VI) reduction to U(V) on exposed surfaces of the underlying GC electrode. This is based on the similarity in the reduction potentials of 0.09V on the bare GC electrode and 0.08V on the GO1 electrode under both methods of loading (i.e. sorption of uranium from solution and pre-adsorption of uranium to GO prior to casting GO on the electrode). These values are shown in Table 2. In the CV plots, the characteristic oxidation (around 0.05V) and reduction (around -0.25V) peaks are accompanied by smaller peaks at +0.21V and +0.13V respectively. The oxidation peak significantly shifts to lower voltage over the duration of the scan while the reduction peaks remain constant but vary in intensity. Based on these CV data, the second chemical species yields a reduction potential of 0.39V when the GO2 electrode was immersed in a U(VI) containing solution and 0.41V when U(VI) was pre-adsorbed onto GO2 prior to casting GO2 onto the electrode. We propose this species also corresponds to U(VI)

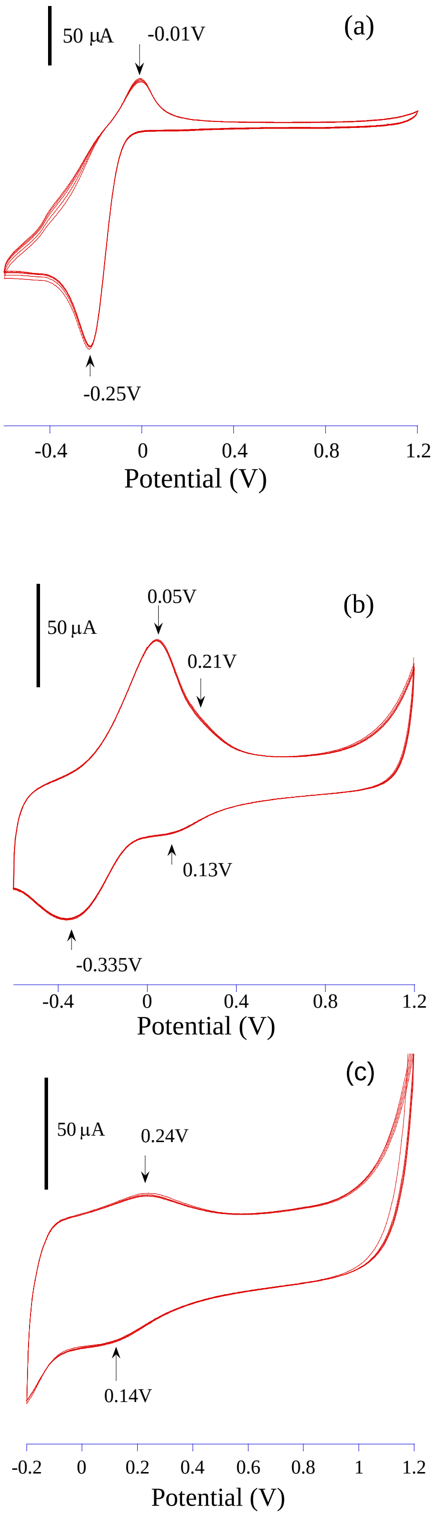

Figure 1. CV curves recorded at 10 mV/s rate for ^{238}U 1mM aqueous solutions with GC (a), GO1 (b) and GO2 (c) working electrodes.

Table 2. Dependence of the reduction-oxidation peaks on the type of the working electrode used in CV experiments (cf. Figure 1 and 2). * Standard reduction potential (relative to hydrogen)

	Initially U(VI) from Solution				**Initially U(VI) adsorbed on GO prior to casting electrode**			
Electrode	ox(V)/ red (V)	E^0_H(V)*	ox(V)/ red (V)	E^0_H(V)	ox(V)/ red (V)	E^0_H(V)	ox(V)/ red (V)	E^0_H(V)
GO1	0.21/0.13	0.39	-0.05/ -0.34	0.08	0.22/0.17	0.41	-0.05/-0.20	0.10
GO2	0.24/0.14	0.41			0.36/0.14	0.47		
GC	-0.01/-0.25	0.09*						

reduction to U(V) but the difference in the reduction potential is due to the uranyl dioxycations coordinating with functional groups on the GO surface which alters the electronic configuration and thus the reduction potentials. A similar result was found for GO2 with a reduction potentials of 0.41V and 0.47V for the two uranium loading methods (Table 2 and Figure 2). As discussed below, ATR-FTIR analysis confirms the presence of U(V) on the GO electrodes following the CV experiments. Reduction of U(VI) to U(V) will occur relatively fast compared with reduction of U(VI) to U(IV) because reduction to the tetravalent state requires breaking of the axial oxygen bonds of the uranyl ion. Therefore, the formation of U(IV) is limited based on the scan rate and conditioning period of the electrode. Thus, due to the relatively fast scan rates relative to the reduction of U(VI) to U(IV), we have primarily examined the U(VI)/U(V) redox couple in this work.

The shape of the voltammetry curves also varies in time indicating transitional processes on the surface of GO1 and GO2 in comparison to the GC electrode, where the redox reactions happen instantly but uranium does not appear to remain sorbed. The duration of the transitional period depends on the type of GO and is much slower in GO1 (commercial sample). Sequential scans with increasing peak intensity during the first two hours of scanning are shown in Figure 2a. The increase in peak intensity is attributed to the accumulation of uranium on the GO surface. In addition to the increase in peak intensity, a small but well pronounced shift in the redox potential values are observed. Moreover, the original (fresh) GO1 electrode exhibits an additional redox couple at +1.1V/+0.8V, which disappear after about one hour of a "conditioning" process. Based on previous CV studies of graphitic materials this redox couple can be assigned to carbon monoxide/carbon dioxide oxidation/reduction processes.[20] This redox couple was also observed during conditioning of the GO1 electrode in uranium free NaCl electrolyte, and is thus unrelated to the uranium-electrode interaction, and will not be discussed further.

For scans using the GO2 electrode, the transitional process is very short (less than 10 min), which makes it difficult to study by voltammetry (i.e., characteristic redox peaks appear almost instantly within several seconds after the commencement of the CV experiments). We hypothesized this increase in intensity is due to the sorption of uranium ions on the surface of the GO1 electrode, which we subsequently confirmed by running additional CV scans using the same electrode in uranium free (0.1 M sodium chloride electrolyte) after it was used in CV scans in a 1 mM uranium solution (Figure 2b). With no uranium present in the aqueous phase, desorption of uranium from the GO1 electrode occurs, which is manifested as a decrease in the peak intensity. The desorption is also accompanied by some conditioning (0.8V reduction peak) as well a slight shift in the uranium oxidation and reduction peak positions for the first 20 minutes of the CV scanning. The results are summarized in Table 2 and show both sorption and desorption of uranium on both types of GO surfaces.

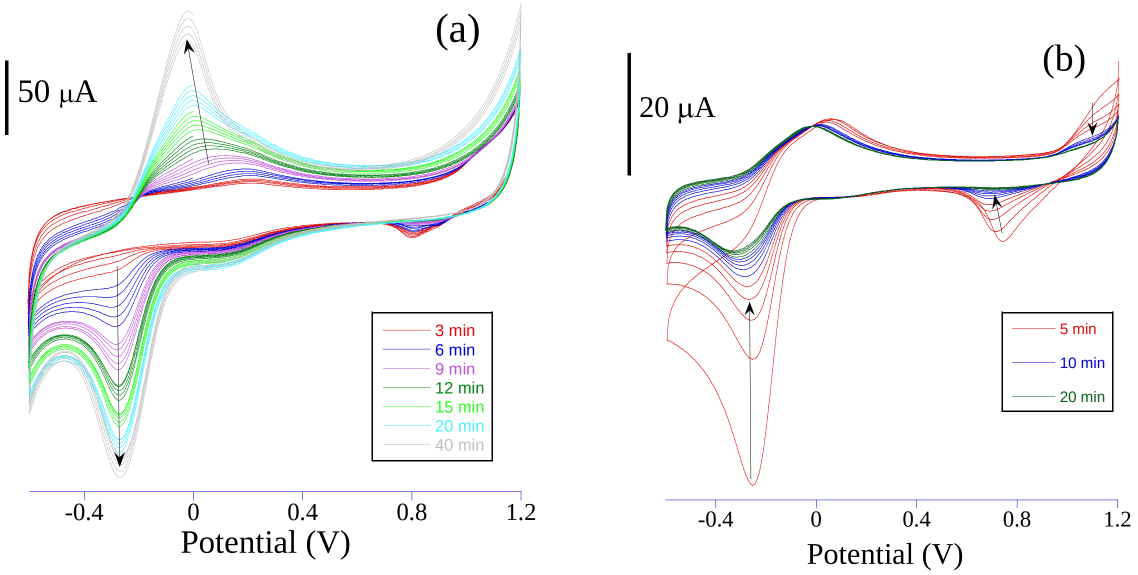

Figure 2. (a) Time evolution of the CV plots during the sorption process of ^{238}U (1 mM solution) with the GO1 working electrode. (b) Same as (a) but now with the GO1 working electrode with pre-adsorbed uranium in uranium free NaCl electrolyte, which corresponds to the desorption process. Scanning rate 100 mV/s. Arrows show the trends in variation of the peak intensities and positions.

Both adsorption/desorption reactions as well as oxidation/reduction reactions of uranium on the GO electrodes were reversible. No discernable signal was recorded with either electrodes in a uranium free NaCl implying that the observed peaks (with 1 mM uranium solution or with pre-adsorbed U(VI) on the electrode) are indeed due to uranium-GO interactions. Slight differences between the redox potentials measured during uranium sorption and desorption are evident, which can be observed more clearly when voltammograms are normalized to the maximal current corresponding to the oxidation peak (Figure 3). First, the oxidation peak position for desorption experiments (i.e., when the uranium is first pre-adsorbed on the electrode and then washed out during CV scanning in NaCl electrolyte) is shifted to a smaller value in comparison to the peak observed when sorption of uranium from the electrolyte solution is occurring. Second, the difference between desorption-adsorption peaks, which is a potential demonstration of “desorption hysteresis”, is higher for the GO2 electrode. Finally, the peak width also appears to be dependent on the type of GO electrode with GO2 sample showing broader peak in comparison to GO1. These changes in the redox potentials and peak characteristics are attributed to uranium interactions with the various functional groups on the GO surface. Since the GC

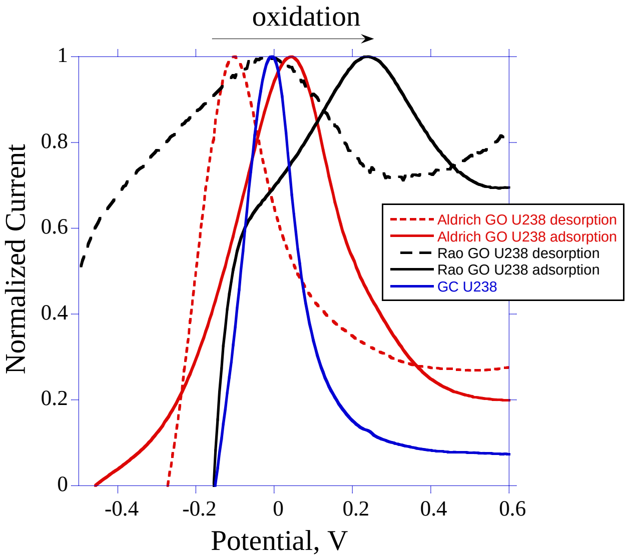

Figure 3. Normalized CV voltagramms (oxidation ramps only) showing variation of the uranium oxidation peak position depending on the adsorption-desorption history and the type of the working electrode. The shift in peak position on nanostructured GO electrodes relative to the GC electrode is proposed to be due to sorption-desorption hysteresis wherein the surface bound species of uranium is changing depending on either sorption or desorption dominating the flux of uranium to or from the electrode.

electrode is not functionalized, the previously reported redox potential of aqueous UO_2^{+2}/UO_2^{+} reactions could be readily measured. However, the coordination of uranium with the functional groups (carboxylate, hydroxide, and potentially sulfonate functional groups), which are present on the GO1 and GO2 surfaces, leads to a change in the U(VI)/U(V) redox potential. Similar changes in aqueous species for carbonate, hydroxide, and sulfate complexes of uranium have been previously observed.

Uranium sorption to the GO was also monitored by ATR-FTIR spectroscopy. Different degrees of functionalization of the GO was observed between the GO1 and GO2 materials. XPS analysis yielded the oxygen-containing functional group distributions presented in Table 1 and the Supporting Information File. ATR-FTIR spectroscopy (Figure 4) substantiated the presence of epoxide groups (~880 cm^{-1} ring deformation; 1305 – 1275 cm^{-1} ring-stretch), phenolic alcohol groups (~1175 cm^{-1} C-OH stretch), and protonated carboxylic groups (1733 – 1710 cm^{-1} C=O stretch). It should be noted however, that many functional groups absorb in this region and the XPS data is necessary to confirm in the presence of such groups. Both GO1 and GO2 exhibited a strong peak near 1050 cm^{-1}, which is likely a sulfoxide group resulting from the sulfuric acid used in the Hummer’s method. The GO1 material also presents evidence of sulfonate groups, an asymmetric S=O stretch at 1395 cm^{-1} and a symmetric stretch at 1220 cm^{-1}. Both materials also showed the presence of some residual water, resulting in the O-H scissoring mode near 1630 cm^{-1}. Uranyl molecules exhibit a characteristic asymmetric stretching vibration whose energy is dependent on the oxidation state of the uranium. $U(VI)O_2^{2+}$ will exhibit an intense stretch between 960-920 cm^{-1} and reduction of $U(VI)O_2^{2+}$ to $U(V)O_2^{+}$ will result in a downshift of this vibration to approximately 820 cm^{-1}.[22,23] Any further reduction of uranium will result in the loss of the axial oxygen atoms and therefore the loss of the characteristic uranyl stretch.

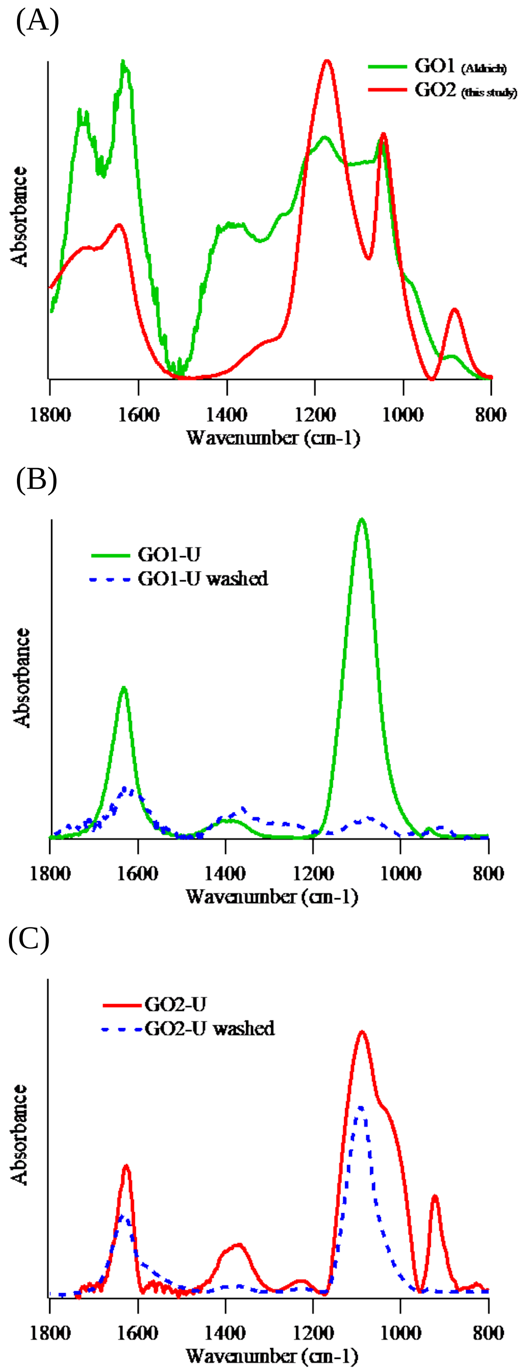

Figure 4. (a) ATR-FTIR spectra of raw GO1 and GO2 films; comparison of ATR-FTIR spectra for GO1 (b) and GO2 (c) samples after deliberate adsorption of uranium from 1mM ^{238}U solution and after its washing with a sodium perchlorate (0.1 M) aqueous solution.

Figure 4b and 4c do show the appearance of these U(VI) and U(V) uranyl stretching peaks, though very weak, in comparison to the two dominant peaks at around 1070 and 1630 cm^{-1} which can be ascribed to a hydroxide form of the uranyl, so-called scheopite type structure $(UO_2)_8O_2(OH)_{12}{\bullet}12(H_2O))$.[24] We hypothesize that the precipitate formed as a result of the presence of aqueous uranyl ions during drying the sample for the ATR-FTIR measuremenst and that the precipitate was not present during the CV scans. This is based on previous observations that the solid can be easily removed from solid surfaces with washing.[24] Uranyl stretches were observed also on the both GO electrode surfaces after exposure to CV scanning with the 1mM ^{238}U electrolyte. In addition to uranyl stretches at 820 cm^{-1} and 943 cm^{-1}, strong overlapping peaks were observed on the GO surfaces after CV scanning at 1011 cm^{-1} and 1092 cm^{-1}. These peaks are similar to those previously identified as the uranyl hydroxide $\gamma_{U\text{-}O\text{-}H}$ bending mode. The peak at 1092 cm^{-1} was observed on both GO surfaces, while the 1011 cm^{-1} was apparent only on the GO2 surface. Both GO surfaces were washed with 0.1 M sodium chloride or 0.1 M sodium perchlorate to investigate the stability of the observed uranium surface species. The shoulder at 1011 cm^{-1} was removed by the washing step. Emerson and Powell[24] attributed this behavior to a uranyl precipitate. The $U(VI)O_2^{2+}$ peak at 920 cm^{-1} was also removed by this washing step, suggesting the precipitate is a uranyl hydroxide, with a $\gamma_{U\text{-}O\text{-}H}$ bending mode. The more refractory $\gamma_{U\text{-}O\text{-}H}$ bending mode observed at 1092 cm^{-1} was not removed from the GO2 surface by the washing step, suggesting it is the result of a uranyl adsorbed to the GO surface. The intensity of the 1092 cm^{-1} peak on the GO2 surface was similar before and after washing. Contrarily, on the GO1 surface the $\gamma_{U\text{-}O\text{-}H}$ bending mode at 1092 cm^{-1} was drastically reduced after washing. The GO2 surface therefore appears form stronger surface complexes with uranyls than the GO1 surface. We propose this to be the manifestation of the higher availability of functional groups on the high-defect monolayer morphology of the GO2 material, as compared to the multilayer morphology of the GO1 material.

Interestingly, adsorption of uranyl leads to an enhancement of the carboxylic group vibration (1630 cm^{-1}), which is practically indistinguishable from background on a uranium free GO1 or GO2 electrodes due to the adsorbed water. Thus, it can be concluded that the uranyl is most likely interacting with the carboxylate functional groups, and consistent with the generally high stability of uranyl carbonate complexes in aqueous systems.[25] At the same time, the epoxide or phenolic groups can act as an additional anchor sites during the adsorption process. Coordination of uranium with carboxylate groups is also in agreement with DFT calculations, which show that –COOH groups form much stronger surface complexes with U(VI) than other oxygen containing functional groups on the GO surface.[26] Based on the current data as well as previous experimental and theoretical considerations, it appears that uranium adsorbs to GO via inner sphere rather than outer sphere complexation with a direct bond with carboxylate functional groups. The former is responsible for the high sorption of U(VI) due to its interaction with the surface carboxylic groups, while the latter promotes complexation with edges on the GO sheet.[26]

The shifts in redox potential of uranium on the two GO electrodes used in this work can be explained by the differences in the surface functional groups of the GO electrodes relative to the GC electrode. Furthermore, differences in the behavior of GO1 and GO2 could be due to differences in their morphology. In comparison to the GC electrode, the GO electrode surfaces raise the reduction potentials which make both the oxidation and reduction reactions more energetically favorable. This phenomenon can be observed in Figures 1 and 3 as a higher shift of the corresponding redox peaks (standard reduction potential values, E^0_H). This could be due to physical differences such as intercalation versus surface adsorption or due to uranium interacting with multiple functional groups on the GO electrode surface (e.g., hydroxide, carboxylic, or sulfonic). Importantly, the reduction potentials on GO1 and GO2 are significantly different from that measured with the GC working electrode, indicating crucial role of the surface functionalization in controlling surface speciation (and thus redox potential of the surface complexes). It is known that the differences in surface functionalization and defects in graphene may perturb the electronic energy levels and the density of states thus leading to different reduction potential while interacting with uranium species.[27,28]

Though this work has proposed to study the U(VI)/U(V) couple, the observed single reduction peak may also correspond to a concept of disproportionation of U(V) to U(IV) and U(VI) during the reduction process discussed in literature.[29-32] The intermediate, U(V) state of uranium is traditionally considered to be unstable and can disproportionate to U(VI) and U(IV).[29-32] However, our experiments are giving an evidence of possible stabilization of this valence state at the GO surface based on the ATR-FTIR measurements. It is quite possible that formation of hydrogen bonds between adsorbed uranyl hydroxide species or some other cooperative effects predicted by theoretical modeling of interactions at GO-water interface are involved.[33] Based on the slow kinetics of U(VI)/U(IV) reaction rates relative to U(VI)/U(V) rates as discussed above, the single reduction peak is proposed to be due to the U(VI)/U(V) coupled. Furthermore, it is noteworthy that disproportionation of U(V) requires that two U(V) atoms interact. However, upon sorption to the GO surface the U(V) dioxycations may be isolated and unable to interact. The counter-argument to this hypothesis is that concentration of U(V) dioxycations is increased near the surface during the desorption step observed in Figure 2b which could facilitate disproportionation. However, the resulting U(IV) would adsorb to the GO surface and peaks corresponding to U(IV) oxidation would be observed. Overall, there is still a lack of comprehensive understanding of uranyl sorption mechanisms and this work can be considered as additional support of the importance of electrostatic interactions in this process.

CV voltammograms show irreversible changes, which cannot occur in the solution only and should involve strong interaction of charged uranium species with the surface. Enhancement of carboxylic group vibrations (Figure 4) stipulates that these particular functional groups might be coordinated with the uranium. Furthermore, the ion-accessible surface area of GO2 material is at least 25-30 times higher than in GO1 as evident from areal capacitance measurements (see Supporting Information file) and, therefore, all functional groups should be readily available. On contrary, the multilayer nature of the GO1 material requires surface diffusion and intercalation process must compete with strong coordination of the uranyl species to the abundant surface. Therefore, we propose the difference in the CV and FTIR data indicates a two-step adsorption process whereby sorbing uranyl molecules are first coordinated with easily accessible carboxylic groups and then either interact with phenolic or sulfonic groups on the surface or precipitate to a scheopite type structure as indicated by the FTIR measurements and similar to the processes reported for other solid surfaces.[34,35] such particles can be detected by transmission electron microscopy or X-ray absorption fine structure (XAFS) experiments.[36] Our preliminary electron microscopy combined microanalysis study did not reveal presence of the uranyl solid state on the sample surface. The rates of this two-step process vary between GO1 and GO2 due to the requirement of the ions to migrate into the bulk structure of GO1, which is consistent with the much faster reaction rates observe on GO2. A more detailed characterization will be required in the future in order to shed light on the exact mechanisms and specific structural organization of adsorbed uranyl. However, such examination goes beyond the scope of the present paper.

Conclusions

The redox reactions of uranium ions on the surface of GO electrodes have been studied by a combination of voltammetry and IR spectroscopy. The applied techniques revealed and highlighted the difference in GO's surface functionality depending on the preparation route. Particularly, the GO voltammetry data indicates a shift in the U(VI)/U(V) reduction potential when coordinated to the GO surface relative to the aqueous U(VI)/U(V) ions. Sorption and intermolecular interactions on the surface of GO electrodes is also supported by the observed different values of the CV oxidation and reduction peaks recorded during and after ^{238}U electrolyte exposure. We report on a slow adsorption/desorption process of U ions into GO particles during CV experiments when a multilayer Aldrich GO1 sample has been used as a working electrode. A few layer sample, GO2, prepared in our lab is characterized with a defective highly ion-accessible surface structure. As a result, uranium exhibited more rapid sorption and desorption behavior and a small shift in the U(VI)/U(V) reduction potential on GO2 relative to GO1. ATR-FTIR confirms presence of residual U(VI) and U(V) on both GO electrodes after CV experiments indicating that some fraction of strongly bound uranium is resistant to desorption and remains at the electrode surface at the end of each experiment despite a significant reduction in the amount of adsorbed uranium. Stabilization of U(V) even after the CV experiments concluded indicates sorption to GO may prevent disproportionation of U(V) which readily occurs in solution. However, more detailed studies are required to verify this phenomena which are beyond the scope of this work.

Our findings demonstrate versatility of the applied approach to monitor the redox speciation of uranium at a novel solid:water interface and examine how surface complexation can control the stability of various redox states. Though mainly qualitative at this point, the approach has a great potential for application to different ions as well as for the advancement to a quantitative technique in the future.

Acknowledgements

This research is funded by the Office of Basic Energy Sciences of the U.S. Department of Energy as part of the Heavy Element Chemistry Program (DE-SC0010355). Authors thank Ms. Jingyi Zhu for her help in electrochemical experiment setup and Prof. Lindsay Shuller-Nickles for giving access to her experimental facilities.

Supporting Information

Results of X-ray fluorescence spectroscopy and X-ray diffraction studies of various types of graphene oxide samples under study; the procedure of the areal capacitance calculation based on CV voltammogram background current.

AUTHOR INFORMATION

Corresponding Authors

*Email: bpowell@clemson.edu, vblizny@clemson.edu, phone: (864) 656-1004

342 Computer Court, Anderson, SC 29625

Author Contributions

The manuscript was written through contributions of all authors. All authors have given approval to the final version of the manuscript.

References

1. A.Adamantiades and I. Kessides, *Energy Policy*, 2009, **37**, 5149-5166.

2. E. S. Craft, A. W. Abu-Qare, M. M. Flaherty, M. C. Garofolo, H. L. Rincavage, and M.B. Abou-Donia, *J. Toxicol. Env. Heal. B,* 2004, **7**, 297–317.

3. F. Belloni, C. Kütahyali, V.V. Rondinella, and A. Mangione, *Environ Sci. Technol*., 2009, **43**, 1250–1255.

4. A. Schierz and H. Zänker, *Environ. Poll*., 2009, **157**, 1088–1094.

5. W.S. Hummers and R.E. Offeman. *Journal of the American Chemical Society,* 1958, **80**, 1339.

6. D.V. Kosynkin, A.L. Higginbotham, A. Sinitskii, J.R. Lomeda, A. Dimeev, B.K. Price and J.M. Tour, *Nature*, 2009, **458**, 872-876.

7. L. Tang, X. Li, R. Ji, K.S. Teng, G. Tai, J. Ye, C. Wei, and S.P. Lau, *Journal of Materials Chemistry*, 2012, **22**, 5676-5683.

8. T.S. Sreeprasad, S.M. Maliyekkal, K.P. Lisha, and T. Pradeep, *J. Hazard. Mater.* 2011, **186**, 921–931.

9. G. Zhao, X. Ren, X. Gao, X. Tan, J. Li, C. Chen, Y. Huang, and X. Wang, *Dalton Trans.* 2011, **40**, 10945-10952.

10. G. Zhao, J. Li, X. Ren, C. Chen, and X. Wang, *Environ. Sci. Technol.*, 2011, **45**, 10454-10462.

11. S. Yang, Y. Chang, H. Wang, G. Liu, S. Chen, Y. Wang, Y. Liu, and A. Cao, *J. Colloid Interf. Sci*., 2010, **351**, 122–127.

12. T. Xinquan, Y. Xiaobo, L. Songsheng, and W. Mingming, *J. Radioanal. Nucl. Chem.*, 2015, **303**, 245−253.

13. G. Zhao, T. Wen, X. Yang, S. Yang, J. Liao, J. Hu, D. Shao, and X. Wang, *Dalton Trans.*, 2012, **41**, 6182−6188.

14. N. Pan, D. Guan, T. He, R. Wang, I. Wyman, Y. Jin, and C. Xia, *J. Radioanal. Nucl. Chem*., 2013, **298**, 1999−2008.

15. Z. Li, F. Chen, L. Yuan, Y. Liu, Y. Zhao, Z. Chai, and W. Shi, *Chem. Eng. J.*, 2012, **210**, 539−546.

16. A.Y. Romanchuk, A.S. Slesarev, S.N. Kalmykov, D.V. Kosynkin, and J.M. Tour, *Phys. Chem. Chem. Phys.*, 2013, **15** (7), 2321−2327.

17. Y. Xie, E. M. Helvenston, L. C. Shuller-Nickles, and B.A. Powell, *Environ. Sci. Technol*., 2016, **50**, 1821-1827.

18. Y. Si and E. T. Samulski, *Nano Lett.*, 2008, **8**, 1679-1682.

19. Y. Liang, D. Wu, X. Feng, and K. Mullen, *Adv. Mater*., 2009, **21**, 1679–1683.

20. M. Arenz, K. J. J. Mayrhofer, V. Stamenkovic, B. B. Blizanac, T. Tomoyuki, P.N. Ross, and N. M. Markovic, *J. Am. Chem. Soc.*, 2005, **127**, 6819-6829.

21. M. Acik, G. Lee, C. Mattevi, A. Pirkle, R. M. Wallace, M. Chhowalla, K. Cho, and Y. Chabal, *J. Phys. Chem. C*, 2011, **115**, 19761–19781.

22. K. Muller, V. Brendler, and H. Foerstendorf, *Inorganic Chemistry,* 2008, **47**, 10127-10134.

23. H. Qin, T. Gong, Y. Cho, C. Lee, and T. Kim, *Polym. Chem.*, 2014, **5**, 4466-4473.

24. H.P. Emerson and B.A. Powell, *Radiochimica Acta,* 2015, **103**, 553-563.

25. D.I.Clark, D.E. Hobart, and M.P. Neu, *Chemical Reviews,* 1995, **95**, 25-48.

26. Y. Sun, S. Yang, Y. Chen, C. Ding, W. Cheng, and X. Wang, *Environmental Science & Technology,* 2015, **49**, 4255-4262.

27. R. Narayanan, H. Yamada, M. Karakaya, R. Podila, A.M. Rao, and P.R. Bandaru, *Nano Lett.*, 2015, **15** (5), 3067-3072.

28. J.Y. Zhu, A.S. Childress, M. Karakaya, S. Dandeliya, A. Srivastava, Y. Lin, A.M. Rao, and R. Podila, *Adv. Mater*., 2016, **28** (33), 7185-7192.

29. D.E. Morris, *Inorg. Chem.*, 2002, **41**, 3542-3547.

30. G. Nocton, P. Horeglad, J. Pecaut, and M. Mazzanti, *J. Am. Chem. Soc.*, 2008, **130**, 16633–16645.

31. S. Fortier and T.W. Hayton, *Coordination Chemistry Reviews,* 2010, **254**, 197–214.

32. R.J. Silva and H. Nitsche, *Radiochimica Acta*, 1995, **70**-1, 377-396.

33. Q. Y. Wu, J. H. Lan, C. Z. Wang, C. L. Xiao, Y. L. Zhao, Y. Z. Wei, Z. F. Chai, and W. Q. Shi, *Journal of Physical Chemistry A,* 2014, **118**, 2149-2158.

34. D. M. Singer, S. M. Chatman, E. S. Ilton, K. M. Rosso, J. F. Banfield, and G. A. Waychunas, *Environ. Sci. Technol.,* 2012, **46**, 3811−3820.

35. A. K. Burrell, T. M. McCleskey, P. Shukla, H. Wang, T. Durakiewicz, D. P. Moore, C.G. Olson, J. J. Joyce, and Q. Jia, *Adv. Mater.,* 2007, **19**, 3559–3563.

36. A. van Veelen, J. R. Bargar, G. T. W. Law, G. E. Brown, Jr., and R. A. Wogelius, *Environ. Sci. Technol.,* 2016, **50**, 3435−3443.

Graphical Abstract Figure